Electronic Supplementary Information for Dalton Transactions

Supplementary material

Two Novel Halogeno(cyano)argentates with Efficient Luminescence

Xi Liu, Guo-Cong Guo,* Ming-Lai Fu, Wen-Tong Chen, Zhang-Jing Zhang, Jin-Shun Huang

Materials and Instrumentation.

All chemicals except THF solvent were obtained from commercial sources and used without further purification. THF was purified and distilled by conventional methods, and stored under nitrogen before use. Elemental analyses were performed on a Vario EL III elemental analyzer. The FT-IR spectra were obtained on a PerkinElmer Spectrum using KBr discs in the range 4000–400 cm^{-1}. SPM measurements were carried out under ambient conditions using Veeco NS3A-02NanoscopeIIIa Scanning Probe Microscopy in tapping mode. Optical diffuse reflectance spectra were measured at room temperature with a PE Lambda 35 UV-vis spectrophotometer. The instrument was equipped with an integrating sphere and controlled by a personal computer. The samples were ground into fine powder and pressed onto a thin glass slide holder. The $BaSO_4$ plate was used as a standard (100% reflectance). The absorption spectra were calculated from reflectance spectra using the Kubelka-Munk function: $\alpha/S = (1-R)^2/2R$,[1] α is the absorption coefficient, S is the scattering coefficient which is practically wavelength independent when the particle size is larger than 5 μm, and R is the reflectance. Photoluminescence analyses were performed on an Edinburgh FLS920 fluorescence spectrometer. Thermogravimetric analyses were carried out on a NETZSCH STA 449C unit at a heating rate of 10 °C/min under a nitrogen atmosphere. Data were collected on a Rigaku Mercury CCD diffractometer equipped with a graphite-monochromated Mo Kα radiation (λ = 0.71073 Å) at room temperature. The intensity data set was collected with the ω scan technique and reduced by CrystalClear software.[2] The structure was solved by the direct

1 W. M. Wendlandt, H. G. Hecht, *Reflectance Spectroscopy*; Interscience: A Division of John Wiley & Sons: New York, 1966.

2 *CrystalClear*, Version 1.35; Software User's Guide for the Rigaku R-Axis, and Mercury and

methods and refined by full-matrix least-squares techniques. Non-hydrogen atoms were located by difference Fourier maps and subjected to anisotropic refinement. Hydrogen atoms were added according to the theoretical models. All of the calculations were performed by the Siemens SHELXTL version 5 package of crystallographic software.[3] Since the C and N atoms in the bridging CN groups cannot distinguished crystallographically,[4] assignments based on the refinement of their anisotropic thermal parameters have been made for the present compounds.[5]

Jupiter CCD Automated X-ray Imaging System; Rigaku Molecular Structure Corporation: Utah, 2002.

3 *SHELXTL*, Version 5; Reference Manual; Siemens Energy & Automation Inc.: Madison, WI, 1994.

4 J. C. Dyason, P. C. Healy, L. M. Engelhardt, C. Pakawatchai, V. A. Patrick, A. H. White, *J. Chem. Soc., Dalton Trans.* **1985**, 839–844.

5 (a) G.-C. Guo, Q.-M. Wang, T. C. W. Mak, *Inorg. Chem. Comm.* **2000**, *3*, 313–315. (b) G.-C. Guo, T. C. W. Mak, *Angew. Chem., Int. Ed. Engl*. **1998**, *37*, 3183–3186.

Time-dependent DFT calculation Approach Methodology

Calculations on the electronic ground states of the two compounds were carried out using B3LYP density functional theory. 3-21G quality basis sets were employed for all atoms. The ground state geometry was adapted from the truncated X-ray data, $[Ag_{20}(CN)_7Br_{24}]^{11-}$ for **1** and $[Ag_8(CN)_{12}Cl_8]^{12-}$ for **2**. Based on these geometries, time-dependent DFT (TDDFT) calculation using the B3LYP functional was performed. The ground-state B3LYP and excited-state TDDFT calculations were carried out using Gaussian2003.[6] More accurate data could be obtained with more sophisticated theoretical approaches to gain detailed insights into the energy correlation among various electronic states for nontruncated structures.

6 Gaussian 03, Revision B.02, M. J. Frisch, G. W. Trucks, H. B. Schlegel, G. E. Scuseria, M. A. Robb, J. R. Cheeseman, J. A. Montgomery, Jr., T. Vreven, K. N. Kudin, J. C. Burant, J. M. Millam, S. S. Iyengar, J. Tomasi, V. Barone, B. Mennucci, M. Cossi, G. Scalmani, N. Rega, G. A. Petersson, H. Nakatsuji, M. Hada, M. Ehara, K. Toyota, R. Fukuda, J. Hasegawa, M. Ishida, T. Nakajima, Y. Honda, O. Kitao, H. Nakai, M. Klene, X. Li, J. E. Knox, H. P. Hratchian, J. B. Cross, C. Adamo, J. Jaramillo, R. Gomperts, R. E. Stratmann, O. Yazyev, A. J. Austin, R. Cammi, C. Pomelli, J. W. Ochterski, P. Y. Ayala, K. Morokuma, G. A. Voth, P. Salvador, J. J. Dannenberg, V. G. Zakrzewski, S. Dapprich, A. D. Daniels, M. C. Strain, O. Farkas, D. K. Malick, A. D. Rabuck, K. Raghavachari, J. B. Foresman, J. V. Ortiz, Q. Cui, A. G. Baboul, S. Clifford, J. Cioslowski, B. B. Stefanov, G. Liu, A. Liashenko, P. Piskorz, I. Komaromi, R. L. Martin, D. J. Fox, T. Keith, M. A. Al-Laham, C. Y. Peng, A. Nanayakkara, M. Challacombe, P. M. W. Gill, B. Johnson, W. Chen, M. W. Wong, C. Gonzalez, and J. A. Pople, Gaussian, Inc., Pittsburgh PA, 2003.

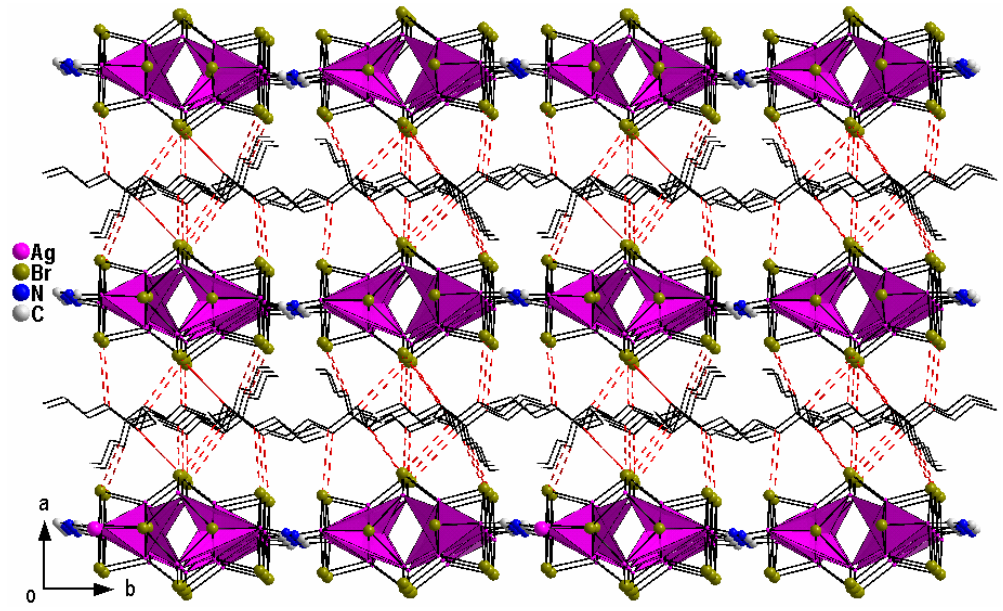

a

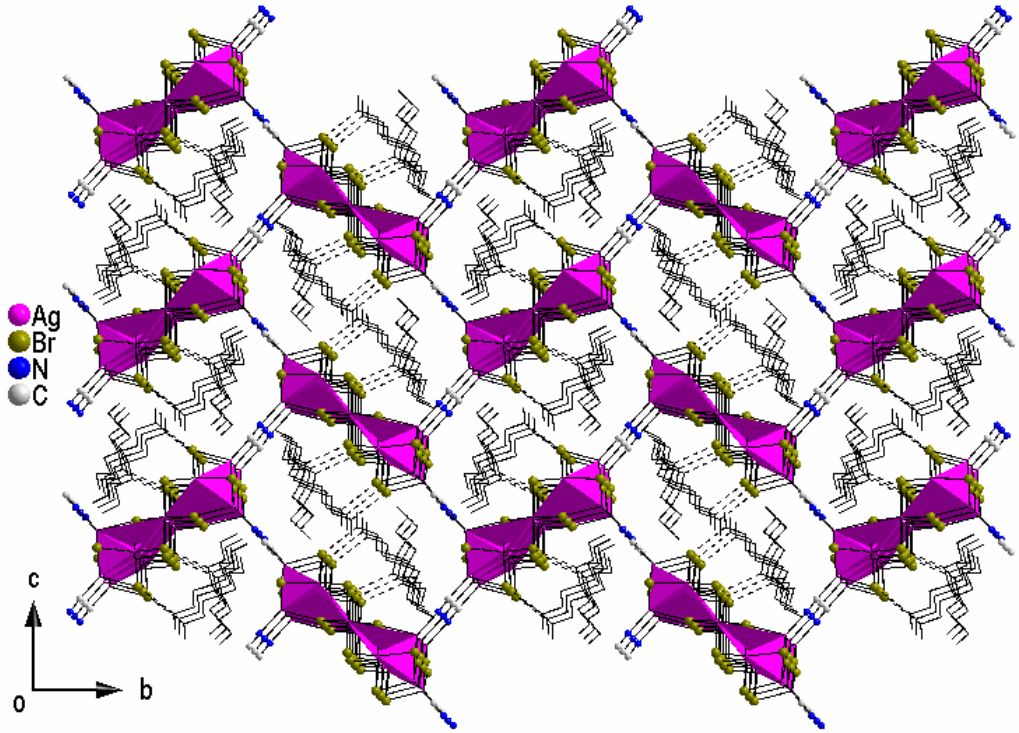

b

Fig. S1 a) The 3-D structure of **1** showing the weak C–H···Br hydrogen bonds (drawn as red dashed lines) between the herringbone-like layers and the $[Bu_4N(3)]^+$ cations. The $[Bu_4N(2)]^+$ cations are omitted for clarity. b) A view of the weak C–H···Br hydrogen bonds (drawn as black dashed lines) within the herringbone-like layers. The $[Bu_4N(3)]^+$ cations are omitted for clarity.

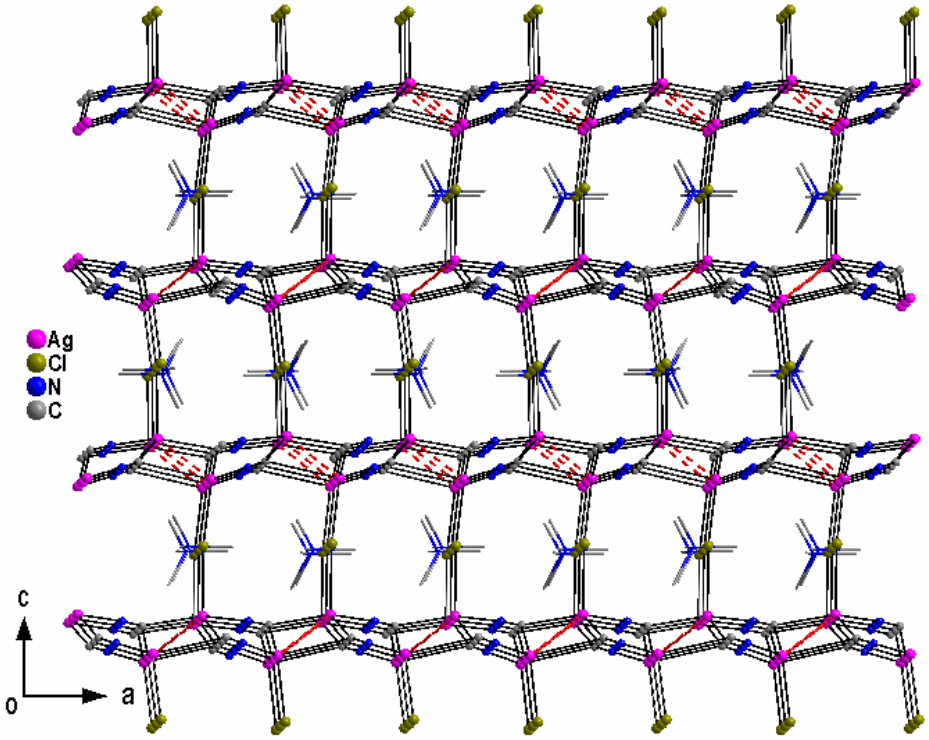

a

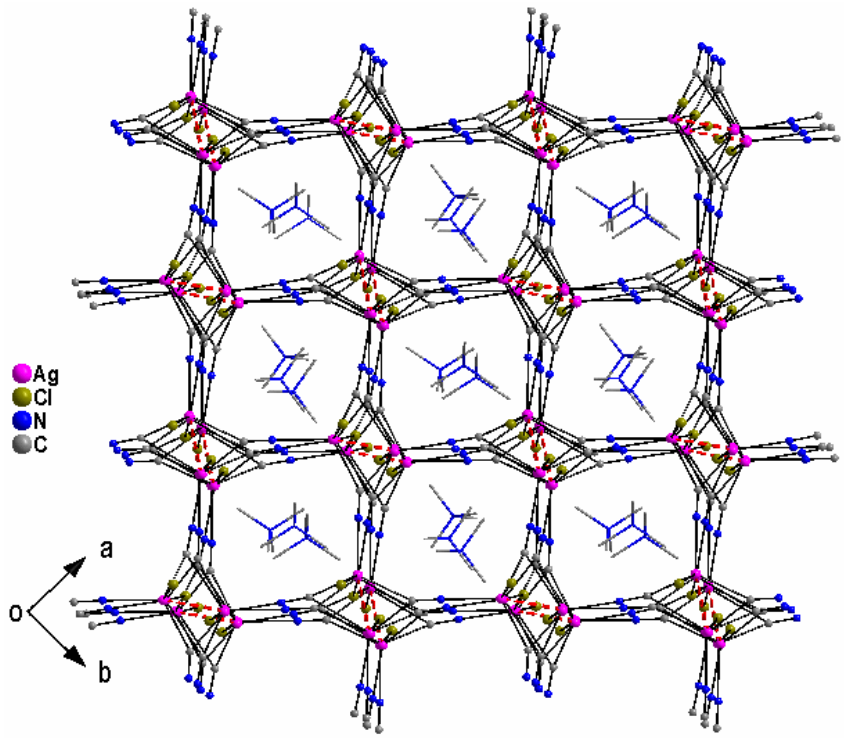

b

Fig. S2 a) A view of 3-D porous framework constructed by μ-chloride atoms connecting the 2-D neutral $^{\infty}_{2}$[AgCN] layers. b) A view of the channels along the *c* axis in **2** in which reside

the $[Me_4N]^+$ cations.

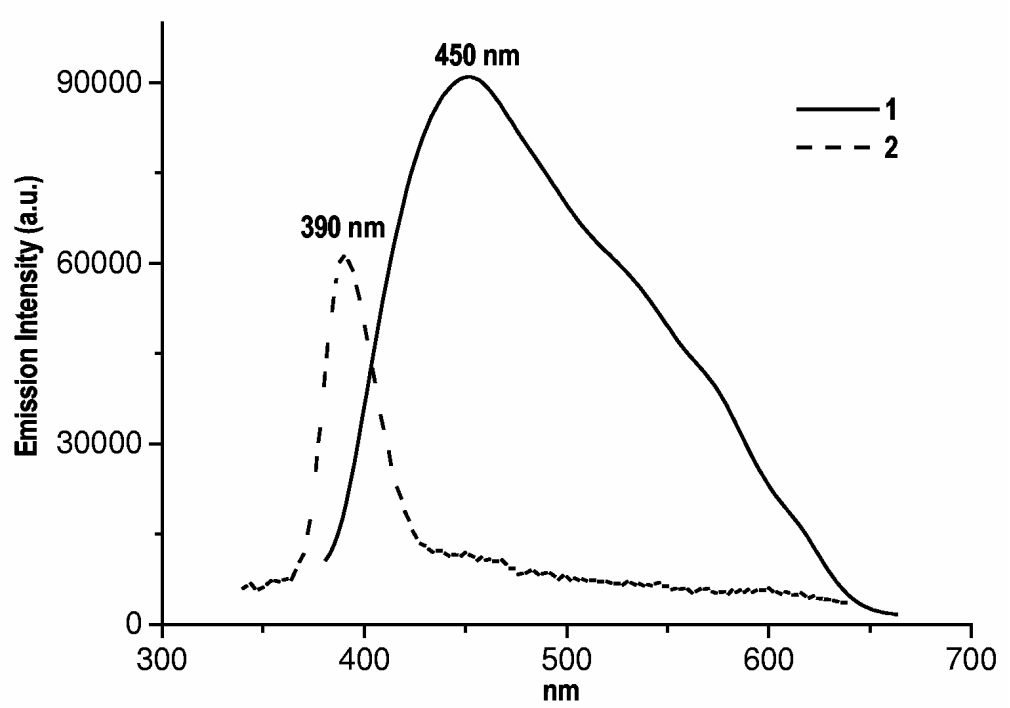

Fig. S3 Solid-state electronic emission spectra of **1** (λ_{ex} = 360 nm) and **2** (λ_{ex} = 330 nm) at room temperature.

	HOMO	LUMO
1	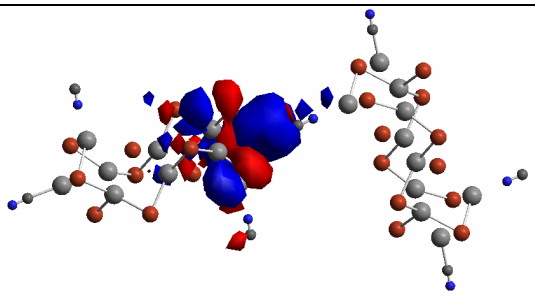	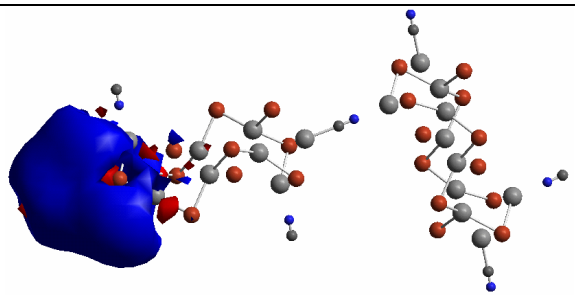
2	HOMO-3	HOMO-1
	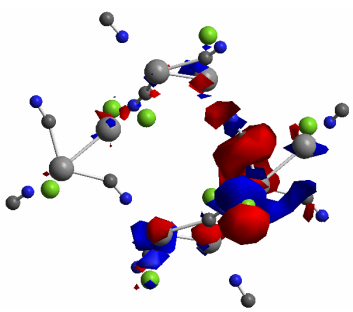	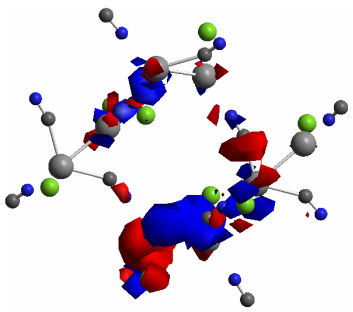

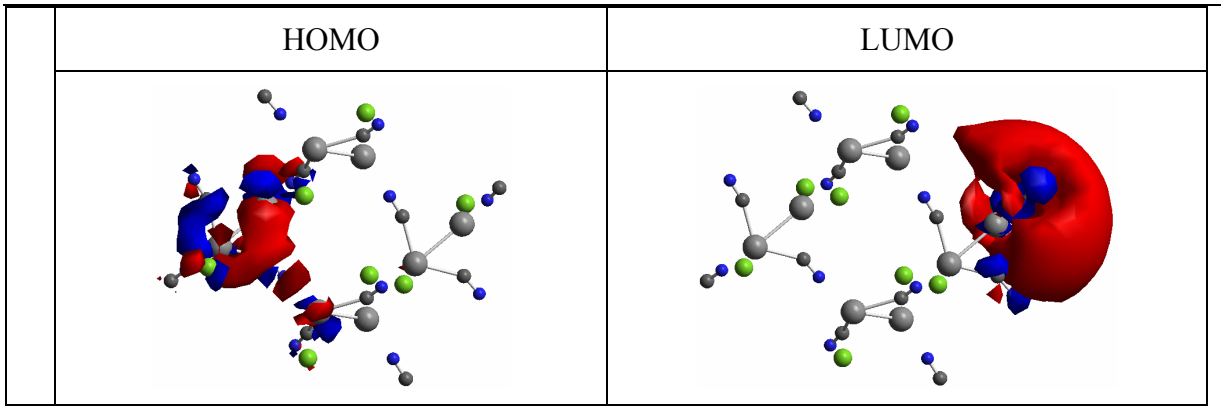

Fig. S4 The electron-density distribution of the corresponding frontier orbitals calculated for **1** and **2**.

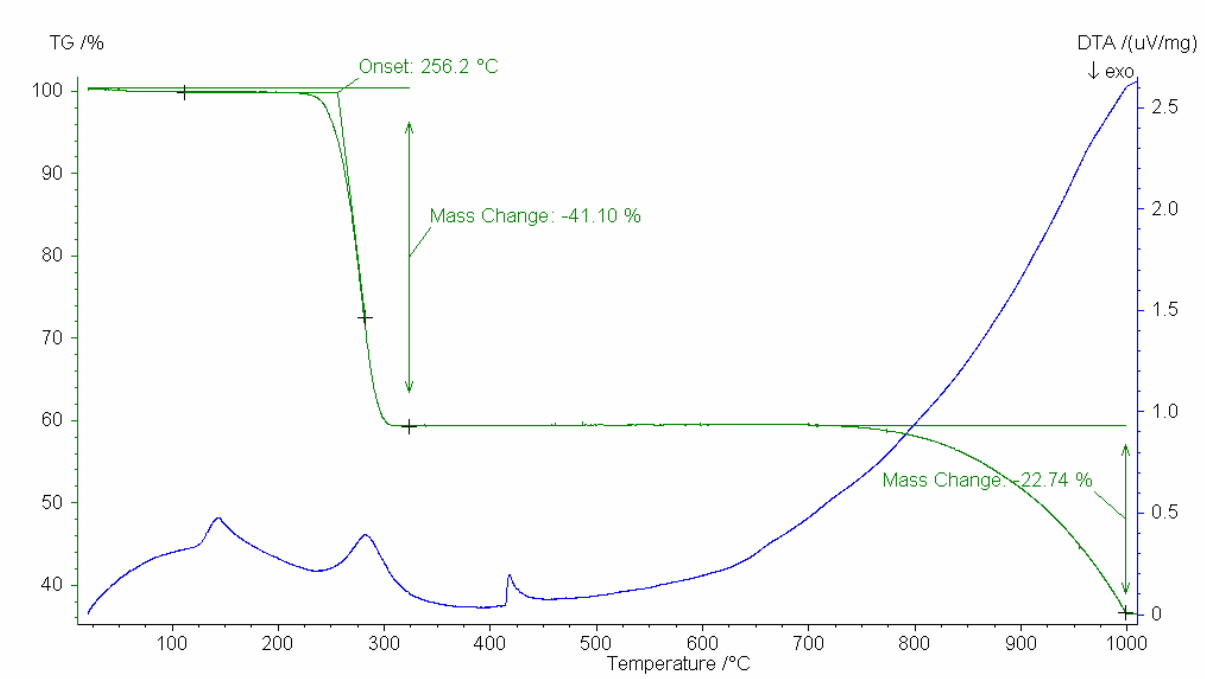

Fig. S5 TGA spectrum of **1** under N_2 atmosphere.

The thermogravimetric analysis (TGA) shows that compound **1** decomposes in two steps with decomposition point T_{onset} of 256.2 °C. The first weight loss is completed at about 310 °C to give a total weight loss of approximately 41.10%, corresponding to loss of two Bu_3N and two BuBr molecules per formula unit (ca. 42.14%). The remainder is calculated to be $Ag_5(CN)Br_4$, which is stable up to 740 °C. The second weight loss finishes at about 1000 °C, giving a total weight loss of approximately 22.74%. The remainder (36.16 %) is calculated to

be silver simple substance (ca. 35.26%). While compound **2** is not very stable at atmosphere and its detailed decomposition mechanisms is very complex which need more correlative experiments to explain the TGA data.

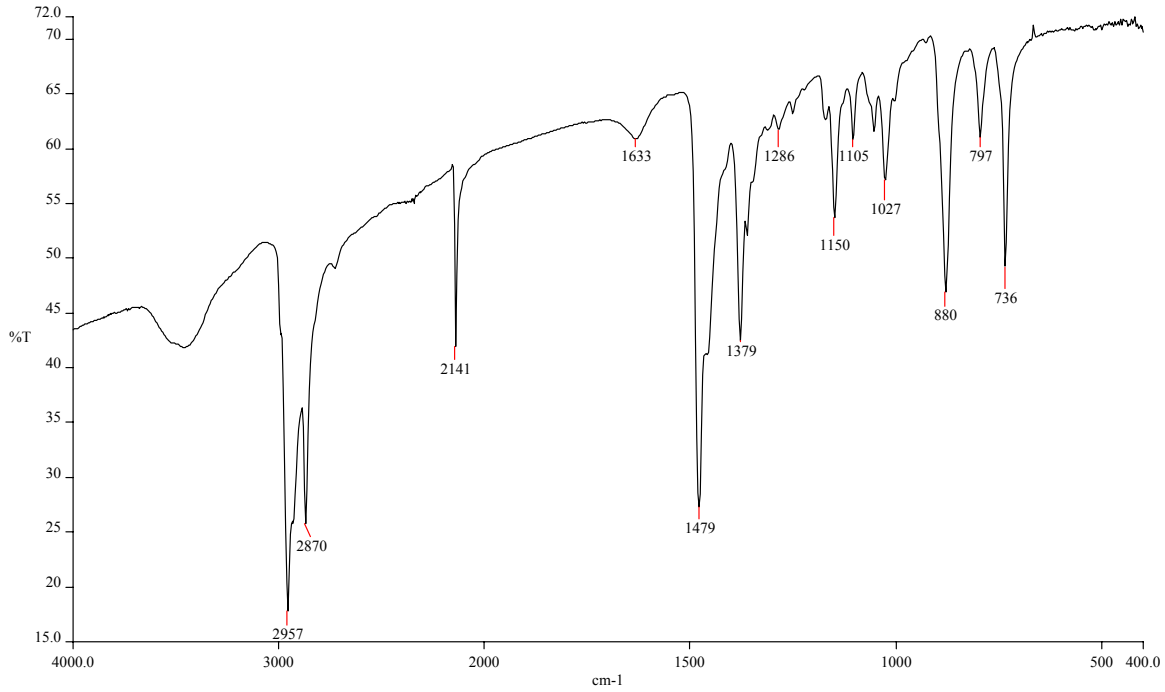

Fig. S6 The IR spectrum of **1** at room temperature.

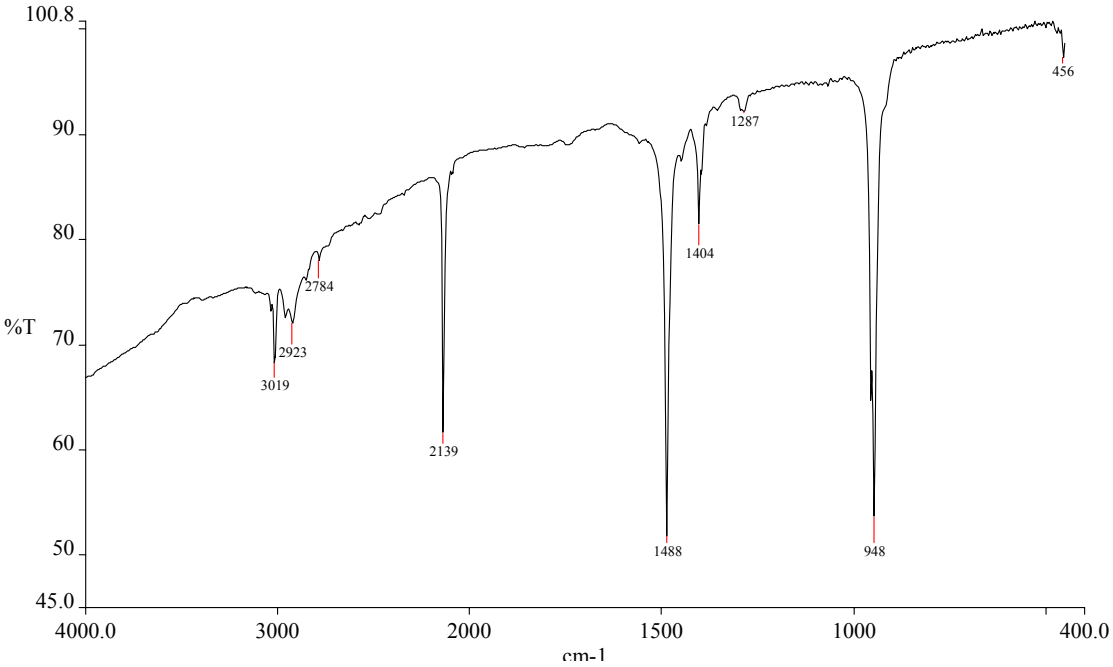

Fig. S7 The IR spectrum of **2** at room temperature.

Table S1. Geometrical characteristics of the C–H···Br hydrogen bonds in **1**.

D–H···A	D–H	H···A (Å)	D···A (Å)	∠(DHA) (°)
C18–H18A···Br5	0.97	2.96	3.822(2)	148.4
C20–H20B···Br5	0.97	2.99	3.829(3)	145.2
C22–H22A···Br4_$1	0.97	2.80	3.638(2)	145.5
C26–H26A···Br6_$1	0.97	2.89	3.842(3)	165.5
C30–H30A···Br3	0.97	3.06	3.823(2)	136.8
C8–H8B···Br1_$2	0.97	3.27	3.786(2)	115.3
C10–H10A···Br6_$2	0.97	3.11	3.837(2)	132.7

Symmetry codes: $1: 1+x, y, z; $2: -x, 1-y, 1-z.

Table S2. The calculated excitation energy (*E*), oscillator strength (*f*), and dominant orbital excitation from TD-DFT calculations for the lowest singlet excitation states.

Compounds	E (nm)	f	Dominant configurations
1	452.21	0.0056	HOMO → LUMO
2	523.97	0.0078	HOMO → LUMO, HOMO-1 → LUMO, HOMO-3 → LUMO